LNF-92/068

Progress report of the machine construction and FEL program on LISA at LNFN

M. Castellano, P. Patteri, F. Tazzioli, J. Zhuang, N. Cavallo, F. Cevenini, F. Cioccci, G. Dattoli, A. Di Pace, G.P. Gallerano, A. Renieri, E. Sabia, A. Torre, L. Catani

Nuclear Instruments & Methods in Physics Research A318 (1992) 168-172

Nuclear Instruments and Methods in Physics Research A318 (1992) 168–172
North-Holland

NUCLEAR
INSTRUMENTS
& METHODS
IN PHYSICS
RESEARCH
Section A

Progress report of the machine construction and FEL program on LISA at LNF

M. Castellano, P. Patteri, F. Tazzioli and J. Zhuang [1]
INFN-Laboratori Nazionali di Frascati, C.P. 13, 00044 Frascati, Italy

N. Cavallo and F. Cevenini
INFN-Sezione di Napoli and Dipartimento di Fisica, Università di Napoli, Pad. 20 Mostra d'Oltremare, 80125 Napoli, Italy

F. Ciocci, G. Dattoli, A. DiPace, G.P. Gallerano, A. Renieri, E. Sabia and A. Torre
ENEA-CRE Frascati, Via E. Fermi, 00044 Frascati, Italy

L. Catani
INFN - Sezione di Roma II, Via E. Carnevale, Roma, Italy

We report the construction progress of the superconducting (SC) linac LISA and of the FEL experiment SURF at LNF. The design criteria of the 25 MeV transport line from the linac to the undulator are presented and the operation and emittance measurements of the 100 keV gun are described.

1. Introduction

The LISA project at LNF was funded by INFN to build a small pilot facility based on a SC accelerator [1]. An IR FEL experiment (SURF), in collaboration with ENEA-CRE Frascati, was later approved and funded [2]. The construction stage is now nearly completed. The accelerator commissioning will start in the near future; both accelerator operation and FEL experimental activity are scheduled to begin in the first half of 1992.

The most relevant parameters of the accelerator and the FEL are listed in table 1.

2. Construction progress of the accelerator

All the components of the accelerator, the power plants and the cryogenic system have been delivered. Orders have been placed for most parts of the 25 MeV transort line at the linac output.

The last months of 1991 will be devoted to commissioning the injector in parallel with the commissioning of the whole cryogenic system and the construction of the 25 MeV transport line.

The 100 keV thermionic gun has been tested in a special setup assembled for emittance measurements, yielding a 1 ms pulse of 200 mA at 100 keV. The normalized rms emittance measured at 90 keV was 8×10^{-6} m rad. These performances fulfill the design requirements.

The 1.1 MeV injector [3] has been fully assembled and is ready for commissioning in the accelerator hall starting in October. Its parts have been laboratory tested at full specification.

The small magnets of the 1.1 MeV arc and spectrometer have been measured; a detailed field map for each magnet has been obtained because large fringe-field effects will probably require an accurate beam transport modelling.

The 4-cell cavity modules have been factory tested in the pulsed regime before delivery. In this mode they provide an average accelerating field greater than 5 MeV/m without quenching, although at lower Q_0 than expected. The measurements of Q_0 vs E_{acc} are shown in fig. 1. CW operation at the design field of 5 MeV/m would require a cooling power exceeding the refrigerator capability. This limitation is expected to be overcome after He processing and RF conditioning. How-

[1] Permanent address: Institute of High Energy Physics, Academia Sinica, Beijing, P.R. China.

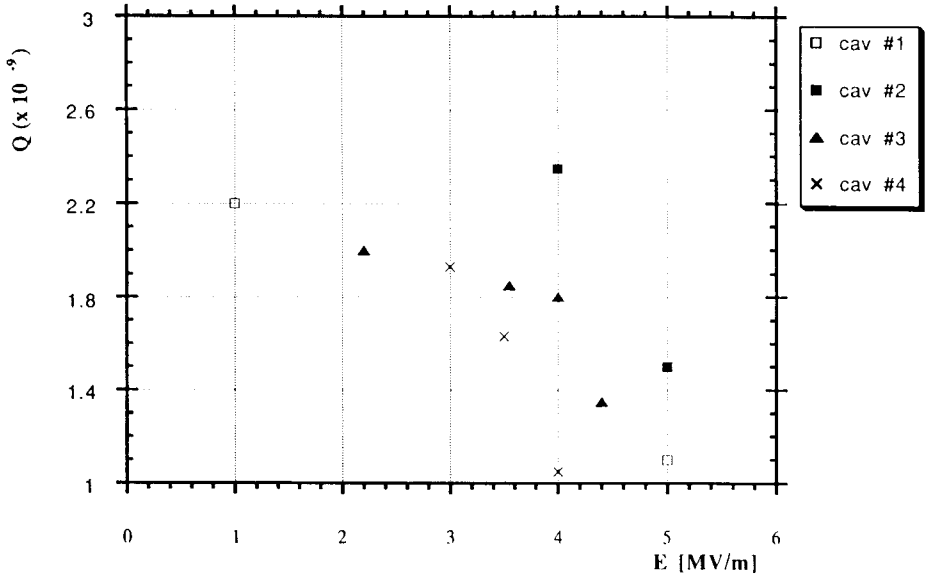

Fig. 1. Plot of Q_0 vs E_{acc} for the four modules of the SC linac.

ever, the performances achieved in the pulse mode satisfy the FEL requirements.

3. Gun test and emittance measurements

Extensive gun tests have been carried out at various anode voltages and beam currents in the pulsed regime at ~ 1 Hz [4], aiming at improving the gun performance and carefully measuring emittance with the fixed-screen variable-focusing method (see fig. 2). The pulse length ~ 1 ms corresponds to the FEL operation mode. The measurements of longer pulses, or at higher repetition rate, were prevented by the excessive beam power hitting the fluorescent screen, causing a harmful pressure rise near the cathode.

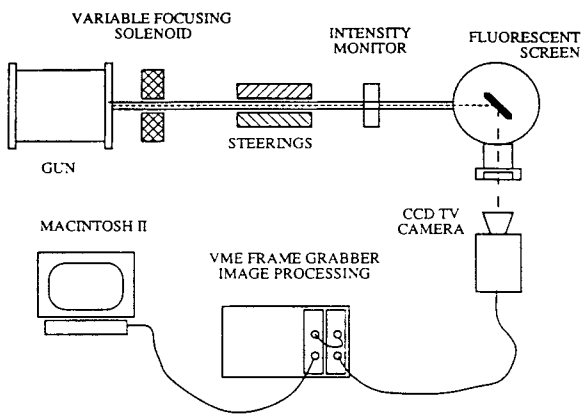

Fig. 2. Experimental arrangement for gun-emittance measurements.

During the preliminary test carried out in the summer of 1990, the gun performance was not fully satisfactory in some aspects. A strong variability of beam size and wandering of position was observed after the first shots of a sequence. This behaviour was due to electrostatic charging of the ceramic gap inserted along the pipe for the toroidal current monitor; an inner metallic shield masking the ceramic from stray electrons completely tamed this instability.

The second shortcoming was current emission saturation at 150 mA, independent of cathode temperature at $T > 1000$°C, well below the maximum cathode emissivity (~ 2 A). Surprisingly, satisfactory emission condition, yielding up to 300 mA, can be achieved at a lower temperature (~ 880°C). This is within a factor of two of the expected temperature-scaled emission. Although this anomalous behaviour is not yet understood, we guess that it is due to surface damage or contamination suffered in the first test run, when a pressure rise up to 10^{-7} Torr and sputtering from the high-sensitivity phosphorous target occurred.

The setup for emittance measurements used a fluorescent screen and a CCD camera. The beam-spot picture was caught by a frame grabber and recorded on disk for off-line analysis. The beam could be monitored shot-by-shot for some time, looking for short- and medium-term misbehaviour. After the aforementioned snags were overcome providing reproducible and stable operation, systematic measurements of beam parameters started. The digitized intensity matrices were

Table 1
Parameter list of the LISA accelerator and FEL

Energy	25 MeV
Bunch length	2.5 mm
Peak current	5 A
Duty cycle	< 2%
Average macropulse current	2 mA
Invariant emittance	10^{-5} π m rad
Energy spread (at 25 MeV)	2×10^{-3}
Micropulse frequency	50 MHz
Macropulse frequency	10 Hz
Undulator periods N	50
Undulator wavelength λ_u	4.4 cm
Undulator parameter K_{rms}	0.5–1.0
Radiation wavelength at 25 MeV	11–18 μm
Linewidth at 15 μm	0.5%
Small-signal gain at 15 μm	9.7%
Small-signal gain at 5 μm (3rd harm.)	2.5%

scanned to compute rms sizes and centre coordinates of each beam spot in both horizontal and vertical directions. From these data, a check of beam size σ and position stability gave $\Delta\sigma/\sigma \sim 1.5\%$ and Δx, $\Delta y < 0.05$ mm.

The emittance ϵ is obtained from the parameters of a fit of beam spot size σ vs the exciting current I_s, i.e., the focusing strength of an upstream solenoid.

The measured dependence of the emittance on current at various anode voltages, is shown in fig. 3. The normalized emittance $\epsilon_n = \beta\gamma\epsilon$ at the nominal operating condition is 8×10^{-6} m rad, consistent with the design parameters.

4. Linac-to-undulator transport line

Beam-quality preservation within the transport line is essential for FEL operation. The FEL gain reduction due to a nonideal beam can be estimated using the accelerator parameters listed in table 1. The reduction factors f reported in table 2 have been derived according to ref. [5]; their values for the design parameters for $\lambda = 15$ μm operation (first harmonic) and 5 μm (third harmonic) are reported in the last two columns.

The factors in the first three lines in table 2 apply to a FEL gain expression that depends linearly on the peak current. The factor $\sigma_{z0}\sigma_z^{-1}$ has been added to the list to explicitly account for the peak-current reduction due to micropulse lengthening.

Space charge and synchrotron emission at 25 MeV affect negligibly the energy spread along the transport line, and the emittance-dependent factors $f(\epsilon_x)$, $f(\epsilon_y)$ would be close to unity even at somewhat worse emittance. Thus the most relevant effect that manifests is the lengthening due to the dispersive property of the channel. Moreover, the lattice of the transport line has to allow easy matching of the beam envelope to the optical mode at various wavelengths, which implies different undulator focussing. Finally, the e^- beam has to be bent toward and away from the optical cavity axis within a short distance from the undulator in order to

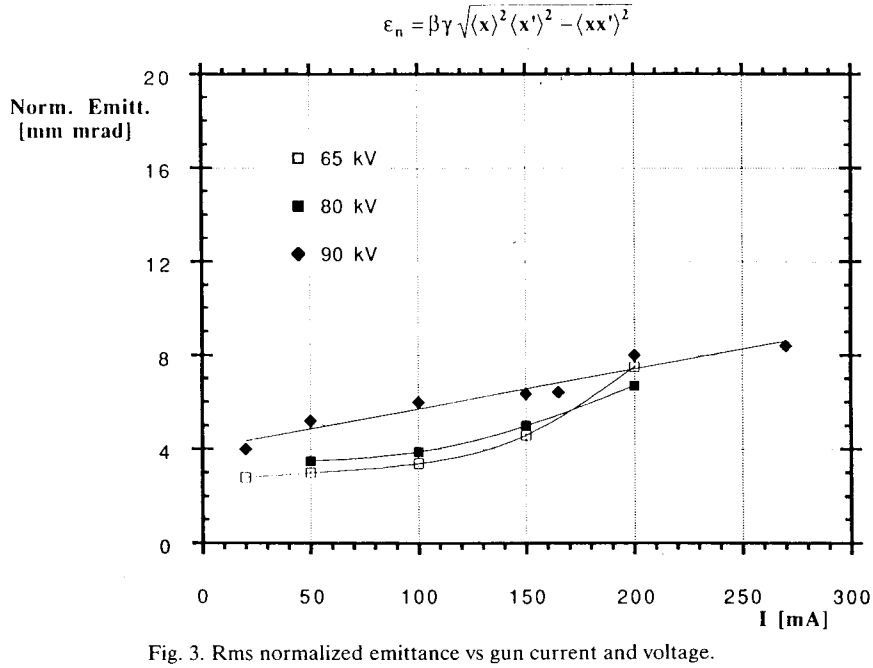

Fig. 3. Rms normalized emittance vs gun current and voltage.

Table 2
FEL gain-reduction factors and their values in LISA-SURF

Source	Parameter	f	at 15 μm	at 5 μm
$\Delta E/E$	$\mu_E = 4N\sigma_E$	$(1+1.7n^2\mu_E^2)^{-1}$	0.79	0.29
Emittance	$\mu_x = 0$	$(1+n^2\mu_x^2)^{-1}$	1.00	1.00
	$\mu_y = 4N\left(\frac{K}{1+K^2}\right)\left(\frac{\gamma\epsilon}{\lambda u}\right)$	$(1+n^2\mu_y^2)^{-1}$	1.00	0.99
Slippage	$\mu_c = N\lambda/\sigma_z$	$(1+\mu_c/3)^{-1}$	0.84	0.84
Pulse lengthening		σ_{z0}/σ_z	0.95	0.95

minimize the mirror separation and to ensure simple alignment and tuning.

The first-order path lengthening in an arc is given by

$$\Delta l = \Delta E/E \int \eta/\rho \, ds, \qquad (1)$$

where the integration is to be computed along the reference trajectory in the bending magnets. In a preliminary study of this transport line, a three-bend lattice was considered. However, it proved to have poor flexibility due to the strong contraints on η required to achive $\Delta l \sim 0$. This forced us to add a matching section and a chicane, composed of two small-angle bending magnets, in order to fulfill all the requirements.

Finally, a three-achromat doublet lattice, without chicane, was preferred. This avoided the use of different magnetic elements while performing satisfactorily in most aspects. The dipoles are sector magnets with a nominal deflecting angle of 30° with $\rho = 0.500$ m, but suitable for 45° deflection when used in the spectrometers. The angle between the entry and exit face is 20°; the wedging angle between the trajectory and the normal to the magnet face is needed to convert part of the horizontal focusing into vertical focusing. Since η, $\eta' = 0$ at one end of each magnet, the overall path lengthening after six magnets, with deflecting angle $\phi = 30°$, is $\Delta l = 6\rho\Delta E/E(\phi - \sin\phi) \sim 140$ μm at $\Delta E/E = 0.2\%$, corresponding to $\sim 5\%$ of the initial micropulse length. Second-order corrections have also been estimated and found negligible.

The optical functions along the arc are plotted in fig. 4. The dispersion-free sections between the doublets allow simple envelope control along the arc. The last magnet steers the beam along the undulator axis. Four quadrupoles and a beam-size monitor in the straight section at the linac output ensure complete control of β and α in both planes at the injection in the arc. A set of stripline monitors (BPM) and steering coils will detect and correct for misalignments of incoming beam. The first magnet of the arc can be separately turned off, leaving the incoming beam to go in the downstream 45° spectrometer magnet. The energy resolution will be 4×10^{-4} at the design emittance. Another spectrometer with similar characteristics will be installed after the undulator to analyze the beam energy spread induced by FEL interaction. Diagnostic devices will be distributed along the arc, the spectrometer lines, and the undulator vacuum pipe. In the first stage, configurations similar to that used for

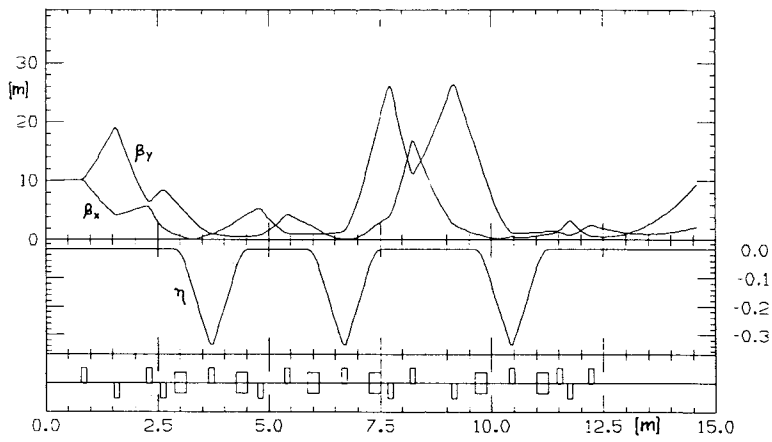

Fig. 4. Optical function along the 25 MeV arc.

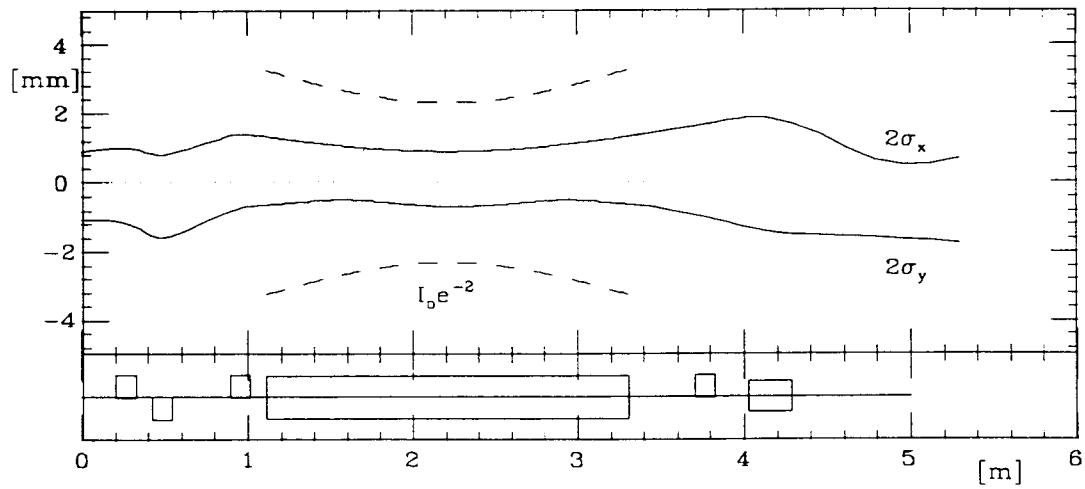

Fig. 5. Beam envelope along the undulator compared with the optical mode profile when set for $\lambda = 15$ μm.

gun emittance measurements are foreseen. Optical-transition radiation screens and synchrotron radiation monitors in the IR are being considered for later developments. The magnetic elements will be provided by Danfysik. The construction of the vacuum chamber diagnostics and ancillary equipments is under way.

5. FEL progress

Assembly of the undulator, a hybrid NdFeB permanent-magnet designed by Ansaldo and ENEA, has been completed. Preliminary measurements indicate an rms variation in field amplitude of 0.3% [6]. Detailed magnetic measurements are under way to tune each period.

The mirror holders and the terminal vessels of the optical cavity are in construction. A test assembly and alignment in air will be carried out before the installation on the beam line.

The beam envelope along the undulator of length $L_u = 2.2$ m has to provide the best overlap between the electron beam and the optical mode. In our cavity, a confocal mode over the undulator length was chosen, i.e. the Rayleigh length $L_R = L_u/2$ [7]. In free space both the e^--beam envelope and optical mode growth from the waist follow a parabolic law $w(z)/w_0 = (1 + z^2/L_R^2)^{1/2}$.

When the sextupolar components of the magnetic field are negligible, the undulator focussing affects the electron beam only in the vertical plane. The previous law for the electron envelope is $\sigma_x = \sqrt{\epsilon\beta_{x0}}\sqrt{1 + z^2/\beta_{x0}^2}$. Matching in the horizontal plane is then obtained with the minimum $\sigma_{x0} = \sqrt{\epsilon\beta_0}$ at the undulator center with corresponding $\beta_{x0} = L_u/2$. In the vertical plane, a matching condition is often imposed so that β_y is an eigenfunction of the undulator period, which ensures a constant envelope along the undulator, neglecting the small modulation with period λ_u. In our case, this criterion gives $\beta_{y0} \sim 0.3$ m since the beam envelope is well within the optical mode up to $\beta \sim 1$ m, the constraints in the vertical plane have been relaxed, so that a quadrupole triplet between the last arc magnet and the undulator ensures a suitable beam envelope in both planes over the full range of the undulator gap. The vertical envelope $(\epsilon\beta_y)^{1/2}$ is drawn in fig. 5 for an undulator parameter K_{rms} corresponding to emission at $\lambda = 15$ μm. The optical mode profile at I_0/e^2 is also shown for comparison.

References

[1] A. Aragona et al., 1988 EPAC Proc. (World Scientific, Singapore, 1989) p. 52.
[2] M. Castellano et al., Nucl. Instr. and Meth. A296 (1990) 159.
[3] A. Aragona et al., 1988 Linear Accelerator Conf. Proc., CEBAF report 89-001 (1989) p. 400.
[4] M. Castellano et al., San Francisco Particle Accelerator Conference, 1991.
[5] G. Dattoli and A. Renieri, in: Laser Handbook, vol. 4 (North-Holland, Amsterdam, 1985).
[6] F. Rosatelli et al., San Francisco Particle Acclerator Conference, 1991.
[7] M. Castellano et al., Nucl. Instr. and Meth. A304 (1991) 204.